AJNR

Enzyme replacement therapy for CLN2 disease: MRI volumetry shows significantly slower volume loss compared to a natural history cohort

Pritika Gaur, Paul Gissen, Asthik Biswas, Kshitij Mankad, Sniya Sudhakar, Felice D'Arco, Angela Schulz, Jens Fiehler, Jan Sedlacik and Ulrike Löbel

AJNR Am J Neuroradiol published online 8 July 2024
http://www.ajnr.org/content/early/2024/07/08/ajnr.A8408

ORIGINAL RESEARCH

Enzyme replacement therapy for CLN2 disease: MRI volumetry shows significantly slower volume loss compared to a natural history cohort

Pritika Gaur,[1] Paul Gissen,[2] Asthik Biswas,[1] Kshitij Mankad,[1] Sniya Sudhakar,[1] Felice D'Arco,[1] Angela Schulz,[3] Jens Fiehler,[4] Jan Sedlacik,[5,6#] Ulrike Löbel.[1#]

ABSTRACT

BACKGROUND AND PURPOSE: Neuronal ceroid lipofuscinoses (NCL) are a group of neurodegenerative disorders. Recently, enzyme replacement therapy (ERT) was approved for CLN2, a subtype of NCL. The aim of this study was to quantify brain volume loss in CLN2 disease of patients on ERT in comparison to a natural history cohort using magnetic resonance imaging (MRI).

MATERIALS AND METHODS: Nineteen (13 female, 6 male) patients with CLN2 disease at one UK center were studied using serial 3D T1-weighted MRI (follow-up time, 1 to 9 years). Brain segmentation was done using FreeSurfer. Volume measurements for supratentorial grey and white matter, deep grey matter (basal ganglia/thalami), lateral ventricles, and cerebellar grey and white matter were recorded. The volume change over time was analyzed using a linear mixed-effects model excluding scans before treatment start. Comparison was made to a published natural history cohort of 12 patients (8 female, 4 male) which was reanalyzed using the same method.

RESULTS: Brain volume loss of all segmented brain regions was much slower in treated patients compared to the natural history cohort. For example, supratentorial grey matter volume in treated patients decreased by 3±0.74% ($p<0.001$) annually compared to an annual volume loss of 16.8±1.5% ($p<0.001$) in the natural history cohort.

CONCLUSIONS: Our treatment cohort showed a significantly slower rate of brain parenchymal volume loss compared to a natural history cohort in several anatomical regions. Our results complement prior clinical data which found a positive response to ERT. We demonstrate that automated MRI volumetry is a sensitive tool to monitor treatment response in children with CLN2 disease.

ABBREVIATIONS: NCL = Neuronal Ceroid Lipofuscinosis, CLN2 = Neuronal Ceroid Lipofuscinosis type 2, TPP1 = tripeptidyl peptidase 1, ERT = enzyme replacement therapy, EMA = European Medicines Agency, ICV = intra-cerebro-ventricular reservoir.

Received month day, year; accepted after revision month day, year.
From the Department of Radiology, Great Ormond Street Hospital, London, UK (PG, AB, KM, SS, FD, UL), National Institute for Health Research Great Ormond Street Hospital Biomedical Research Centre, University College London, London, UK (PG), Department of Paediatrics, University Medical Center Hamburg-Eppendorf, Hamburg, Germany (AS), Department of Diagnostic and Interventional Neuroradiology, University Medical Center Hamburg-Eppendorf, Hamburg, Germany (JF), Robert Steiner MR Facility, Medical Research Council Laboratory of Medical Sciences, Hammersmith Hospital Campus, Du Cane Road, London, UK (JS) and the Mansfield Centre for Innovation, Imaging Sciences, Institute of Clinical Sciences, Imperial College London, Hammersmith Hospital Campus, Du Cane Road, London, UK (JS).

Disclosure of conflicts of interest: Angela Schulz and Paul Gissen have been the recipients of research funding from Biomarin. This work was supported by funding from the United Kingdom Medical Research Council grants MR/N019075/1 and MR/R026084/1 to Paul Gissen. All other authors declare no conflicts of interest related to the content of this article.

Please address correspondence to Dr. Ulrike Löbel, Department of Radiology, Great Ormond Street Hospital for Children NHS Foundation Trust Great Ormond Street, WC1N 3JH London, UK; ulrike.loebel@gmail.com.

SUMMARY SECTION

PREVIOUS LITERATURE: CLN2 is one of thirteen genetically distinct subtypes of human neuronal ceroid lipofuscinoses described to date. Recently, recombinant human tripeptidyl peptidase 1 (cerliponase alfa), an enzyme-replacement therapy has been developed and approved in 2017 for treatment of CLN2 disease after a clinical trial confirmed a significantly reduced decline in motor and language function in treated patients compared to historical controls. Automated MRI volumetry has been used successfully to quantify brain atrophy in a natural history study of CLN2 and CLN3 patients.

KEY FINDINGS: Automated MRI volumetry showed that brain atrophy is significantly slower in CLN2 patients treated with intrathecal enzyme replacement compared to the natural history cohort. The difference in atrophy was most marked for the supratentorial grey matter with an annual 13.8% reduction in volume loss.

KNOWLEDGE ADVANCEMENT: MRI volumetry is a useful, unbiased tool for the assessment of treatment-related response in CLN2 trials. The method is feasible despite the presence of signal dropout from the intra-cerebro-ventricular reservoir by evaluating the contralateral hemisphere only.

Copyright 2024 by American Society of Neuroradiology.

INTRODUCTION

Neuronal Ceroid Lipofuscinoses (NCL) are a group of lysosomal storage disorders characterized by excessive accumulation of lipofuscin in neuronal and extra neuronal tissues,[1] and neurodegeneration. Currently, thirteen genetically distinct subtypes of human NCLs have been identified with variable ages of onset, such as congenital, infantile, late-infantile, juvenile, or adult. The genes affected in NCL encode lysosomal enzymes and other proteins linked to lysosomal functions.[2]

CLN2 disease is caused by pathogenic variants in the *CLN2* gene resulting in a deficiency of the lysosomal enzyme tripeptidyl peptidase 1 (TPP1). TPP1 is a serine protease, deficiency of which results in lysosomal accumulation of a mixture of proteins and lipids.[3] Most patients with CLN2 disease present with the classic late-infantile form of the disease. Delay in language development is usually noticed first, followed by onset of seizures and ataxia between 2-4 years of age and eventually psychomotor, language and visual decline.[4,5]

An increasing number of CLN2 patients present with an atypical phenotype which is characterized by later onset and slower neuro-regression as well as an incomplete combination of symptoms. The atypical CLN2 patients are more difficult to recognize clinically because of disease variability and the time from disease onset to diagnosis is usually longer.

On magnetic resonance imaging (MRI), the natural disease is characterized by progressive infratentorial and supratentorial grey matter atrophy with associated white matter signal abnormalities.[6,7,8] As the disease mainly affects neurons, white matter signal changes are likely secondary and hypothesized to be related to Wallerian degeneration and gliosis.[9,10] Thalamic T2 hypointensity and volume loss have been attributed to the accumulation of saposin and glial fibrillary acid protein containing hypertrophic astrocytes containing storage proteins.[11,12]

Pre-clinical studies were performed in TPP1 deficient mouse and dog models and eventually on children, where intrathecal and intra-cerebro-ventricular (ICV) administration of TPP1 halted the neuropathological features of the disease and slowed disease progression.[13,14,15] In 2017, an enzyme replacement therapy (ERT), 'Cerliponase alfa', was approved for treatment of CLN2 disease by the FDA and European Medicines Agency (EMA) after almost two decades of research and scientific knowledge advancement. The clinical trials were done in four international centers (Hamburg, London, Rome, and Columbus) and showed remarkable slowing in the expected rate of clinical decline based on a visual and motor clinical rating score.[5] In 2019, Cerliponase alfa was approved for reimbursement in the UK for patients diagnosed with CLN2 as part of the managed access agreement.[16] The drug is delivered directly into the intrathecal compartment via an ICV reservoir. As part of the managed access agreement, MRI is performed yearly to assess disease progression or treatment-related changes.

Recently, MRI volumetry has been suggested as a viable biomarker for monitoring disease progression in the neuronal ceroid lipofuscinoses and the good correlation of volume loss described on MRI with the clinical scores.[5,6,17,18] In addition, in a CLN2 miniswine model, MRI brain volumetry has been shown to be highly sensitive to early disease detection.[19]

The purpose of this study was to compare anatomical regional MRI brain volumes of the CLN2 patients treated with ERT at Great Ormond Street Hospital in London, UK to a previously published natural history cohort,[6] and determine if the reported significant clinical effect of therapy in the paper by Schulz et al.[15] can also be detected using MRI on long-term follow-up.

MATERIALS AND METHODS

Twenty-eight patients with CLN2 disease were enrolled in treatment studies at Great Ormand Street Hospital for Children at the time of the imaging analysis. For this retrospective analysis, IRB approval was waived. Three patients without available follow-up imaging, three patients with an atypical form of CLN2 disease, and three patients with extensive imaging artefacts were excluded from the analysis leaving 19 patients (13 female, 6 male) (Supplementary Figure 1). Patient details are summarized in Table 1. Patients commenced treatment at different time points, typically at ages 2 to 5 years. Patients did not receive other treatments apart from anti-seizure medication.

Although CLN2 patients with atypical phenotypes who had evidence of progressive CNS disease were treated with Cerliponase alfa in our center, they have unpredictable disease progression that does not match the natural history cohort and hence they were excluded from this analysis. The patients with unavailable follow-up imaging were enrolled just before the imaging analysis, so no follow-up imaging was yet done (patients G2-3) or follow-up imaging was not commenced for other reasons (patient F3).

Serial 3D T1-weighted MRI of our treated patients were available for baseline and follow-up times ranging from 1 to 9 years. The follow-up period was variable as patients started treatments between 2014 and 2022, with some patients still under follow-up to date.

We compared the brain volume changes under treatment (1-9 years follow-up scans only) to a previously published natural history cohort of 12 patients (8 female, 4 male; observation age range, 2 to 10 years).[6] To be able to compare our results, we reanalyzed the natural history data using the same statistical methods as for our treatment cohort, and recorded the underlying gene mutation (Tables 1 and Supplementary Table 1). We also specifically analyzed the brain volume change for the first year including the baseline scan short before (1-2 weeks) treatment start and all available follow-up scans within the first year under treatment. Eight patients were excluded from this subset as no usable 3D data sets were available for analysis at baseline and within the first year of follow-up (Supplementary Table 2). In addition, MRI results were correlated to the Clinical Motor Language Score.

Imaging

MRI was performed on 1.5 Tesla (n=96) or 3 Tesla (n=10) scanners with most scans done on 1.5T systems. Most children required sedation using general anesthesia to obtain adequate image quality.

The imaging protocol included conventional MRI sequences (FLAIR, T2WI, DWI) and a 3D T1-weighted MPRAGE (n=47) or T1WI GRE (n=59) sequence. The 3D T1-weighted sequences were used for volumetric analysis. The MPRAGE sequence parameters were in the range of: TR = 1500-2300 ms, TE = 2.5-2.7 ms, T1 = 900-1000 ms, flip angle = 8° and the GRE parameters: TR = 11-14 ms, TE = 5-7 ms, flip angle = 15°. Both sequences were acquired in sagittal orientation with a matrix size of 256 x 256 with 150-210 slices and 1 mm

isotropic voxels. 106 scans were available for analysis from 19 patients. We excluded 7 scans from 2 patients due to extensive artefact from the ICV reservoir. In addition, some of the patients did not have useable 3D T1 volumetric datasets at certain imaging time points and therefore 15 scans from a total of 10 patients were excluded from analysis.

A total number of 84 good quality MRI scans were available for our treatment cohort.

Table 1: Patient characteristics including genetic mutations and motor and language scores at the point of commencement of ERT versus the latest scores. The atypical phenotypes were excluded. Other patients (not listed in table) were excluded due to extensive imaging artefacts and due to lack of follow-up imaging.

Demographics (Age at diagnosis/sex)	**ERT start age** (baseline MRI 1-2wks earlier)	**CLN2 (motor+ language) score at ERT start**	**Latest CLN2 (motor+ language) score** (Age)	**Phenotype**	**Mutation**
4y8m/F	4y10m	1+0	0+0 (11y5m)	classical	c89+5G>A/ c.509-1G>C
4y4m/F	4y7m	1+2	0+0 (10y3m)	classical	c.509-1G>C/ c.509-1G>C
2y2m/F	4y	3+3	2+2 (9y)	classical	c.509-1G>C/ c.509-1G>C
4y1m/F*	4y5m	3+2	2+2 (8y)	classical	c.1094G>A/ c.622C>T
4y3m/M	4y5m	2+0	1+0 (10y9m)	classical	c.1052C>T/ c.1052C>T
4y2m/F	4y7m	1+1	0+0 (14y)	classical	c.509-1G>C/ c.509-1G>C
3y11m/M*	4y4m	2+2	1+2 (13y3m)	classical	c.1266 G>C/ c.1266 G>C
3y7m/F	3y11m	2+2	0+0 (13y)	classical	c.509-1G>C/ c.622C>T
0y15m/F*	1y9m	3+3	3+3 (8y)	classical	c89+5G>A/ c.509-1G>C
3y5m/F*	3y11m	3+2	1+2 (6y4m)	classical	c.509-1G>C/ c.622C>T
4y5m/M*	4y9m	1+1	1+1 (8y3m)	classical	c.1678-1679 del/ c.622C>T
7y11m/M	8y5m	2+2	1+2 (12y)	Atypical phenotype	c511G>C/ c.622C>T
4y2m/M*	4y4m	2+1	1+1 (7y5m)	classical	c379C>T/ c.509-1G>C
4y5m/F*	4y8m	2+2	1+0 (6y8m)	classical	c.509-1G>C/ c.509-1G>C
4y5m/F	4y7m	2+2	1+0 (6y11m)	classical	c17+1del/ c.509-1G>C
4y0m/M*	4y2m	2+2	1+1 (6y4m)	classical	c1525C>T/ c.509-1G>C
13y1m/M	13y2m	2+2	2+2 (13y10m)	Atypical phenotype	c.1340G>A/ c.509-1G>C
10y8m/F	10y9m	2+2	2+2 (11y5m)	Atypical phenotype	c.1340G>A/ c.509-1G>C
4y10m/M*	4y11m	2+2	1+1 (5y10m)	classical	c.509-1G>C/ c.509-1G>C
3y10m/F*	3y11m	2+2	1+2 (6y)	classical	c.509-1G>C/ c.509-1G>C
3y1m/F*	3y2m	3+0	3+0 (5y)	classical	c.509-1G>C/ c.509-1G>C
4y3m/F	4y5m	2+2	2+2 (5y)	classical	c.622C>T/c.1645G>A

*These patients were included in the Baseline-to-1-year-follow-up MRI subgroup analysis

Data Processing

The FreeSurfer Software Suite (version 6.0)[24] was used for brain segmentation running the automated recon-all command with the -watershed atlas option for robust skull stripping. The segmentation (i.e., the aseg.mgz files) of all scans which were 3D volumetric T1 sequences were visually checked (Figure 1) for any major segmentation errors (obvious grey and white matter segmentation errors, inclusion of dural venous sinuses and or skull/soft tissue). No manual segmentation correction was done (examples of baseline and follow-up scans in Supplementary Fig. 2.1. and 2.2).

The volume measurements of the segmented brain regions were extracted from the resulting aseg.stats files of each scan for supratentorial grey and white matter, deep grey matter (basal ganglia/thalami), lateral ventricles (including the choroid plexus), cerebellar grey and white matter. These are the same regions analyzed in the earlier published natural history cohort.[6]

Statistical Analysis

The volume changes were first analyzed between the baseline scans 1-2 weeks before treatment start, and all scans acquired during the first year of follow-up. The volume changes were also analyzed only for the 1-to-9-year follow-up scans excluding the pre-treatment baseline scans. Furthermore, the available clinical scores (Table 1, sum of M- and L-scores) were correlated with the supratentorial grey matter volumes of the MRI scans closest to the clinical assessments.

Data analysis was done in R 4.0.4 using the linear mixed-effects model package lme4 version 1.1-33,[20] and the partial correlation package ppcor version 1.0.[21]

The logarithm of the volume measurements was calculated to linearize the exponentially appearing volume loss over time (i.e., patient age) for the analysis. A linear mixed-effects model was calculated, using the syntax of the lme4 package as below, to account for the non-independent multiple follow-up measurements of each patient.

$$\log(\text{region\_volume}) \sim \text{age} + (\text{age} \mid \text{patient})$$

The ppcor package cannot account for the dependency of follow-up measurements of the same patient, therefore all measurements were treated as independent for the correlation analysis.

Due to the susceptibility artefact caused by the ICV reservoir used for drug delivery, only the contralateral hemisphere was included in the analysis of the treatment cohort. This assumes that the volume change with patient age is the same for both hemispheres. The lme4 formula for analyzing the natural history cohort was, therefore, modified to account for a potential effect between the hemispheres as well an interaction with age as follows:

log(region_volume) ~ age * hemisphere_side + (age | patient) + (hemisphere_side | patient).

There was no statistically significant association or interaction with age of the brain volume change between the hemispheres. This allowed us to compare the age effect of the modified analysis of both hemispheres of the natural history cohort with the analysis of the contralateral hemisphere of the treatment cohort which could be either side. The volume measurements over time of both hemispheres of the natural history cohort were also analyzed with the partial correlation analysis to control for potential correlations between the hemispheres. However, no statistically significant correlation was found between the hemispheres. The remaining correlation coefficients with age of that partial correlation analysis of the natural history cohort were used for comparison with the treatment cohort.

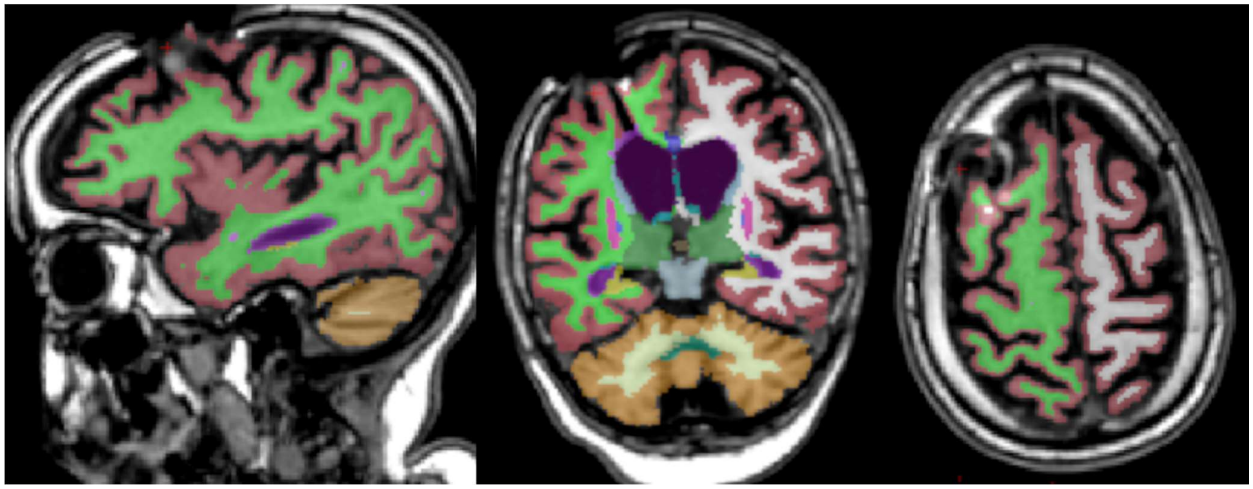

FIG 1. Example of an overlay of FreeSurfer segmentation on a 3D T1 MPRAGE image. Segmentation of supratentorial cortical grey matter (red), supratentorial white matter (green and white) and cerebellar grey (orange) and white matter (yellow) are depicted. In addition, deep grey matter (basal ganglia/thalami) were segmented and analyzed. Note, the susceptibility artefact from the Ommaya reservoir over the right hemisphere. The contralateral hemisphere is used for data analysis.

RESULTS

After exclusion of patients as described above, the treatment cohort consisted of 19 CLN2 patients (13 female, 6 male) which were compared with the published natural history cohort of 12 patients (8 female, 4 male). The age distribution was similar amongst both cohorts. Overall, more female patients were included in both cohorts, but this was even more prevalent in the treatment cohort.

The volume loss between the baseline scans and first year follow-up for our treatment cohort (Supplementary Table 2, left rows; Figure 2, grey symbols and lines) compared to the natural history cohort (Supplementary Table 2, right rows; Figure 2, yellow symbols and lines) were slightly lower for the supratentorial cortical grey and white matter as well as for the cerebellar grey matter, but the basal ganglia/thalami and cerebellar white matter showed a higher rate of volume loss. The lateral ventricles showed a much higher volume increase in the first year on treatment as compared to the natural history cohort. The Pearson correlation coefficients are similar to the natural history cohort, except for the supratentorial cortical white matter where it is close to zero.

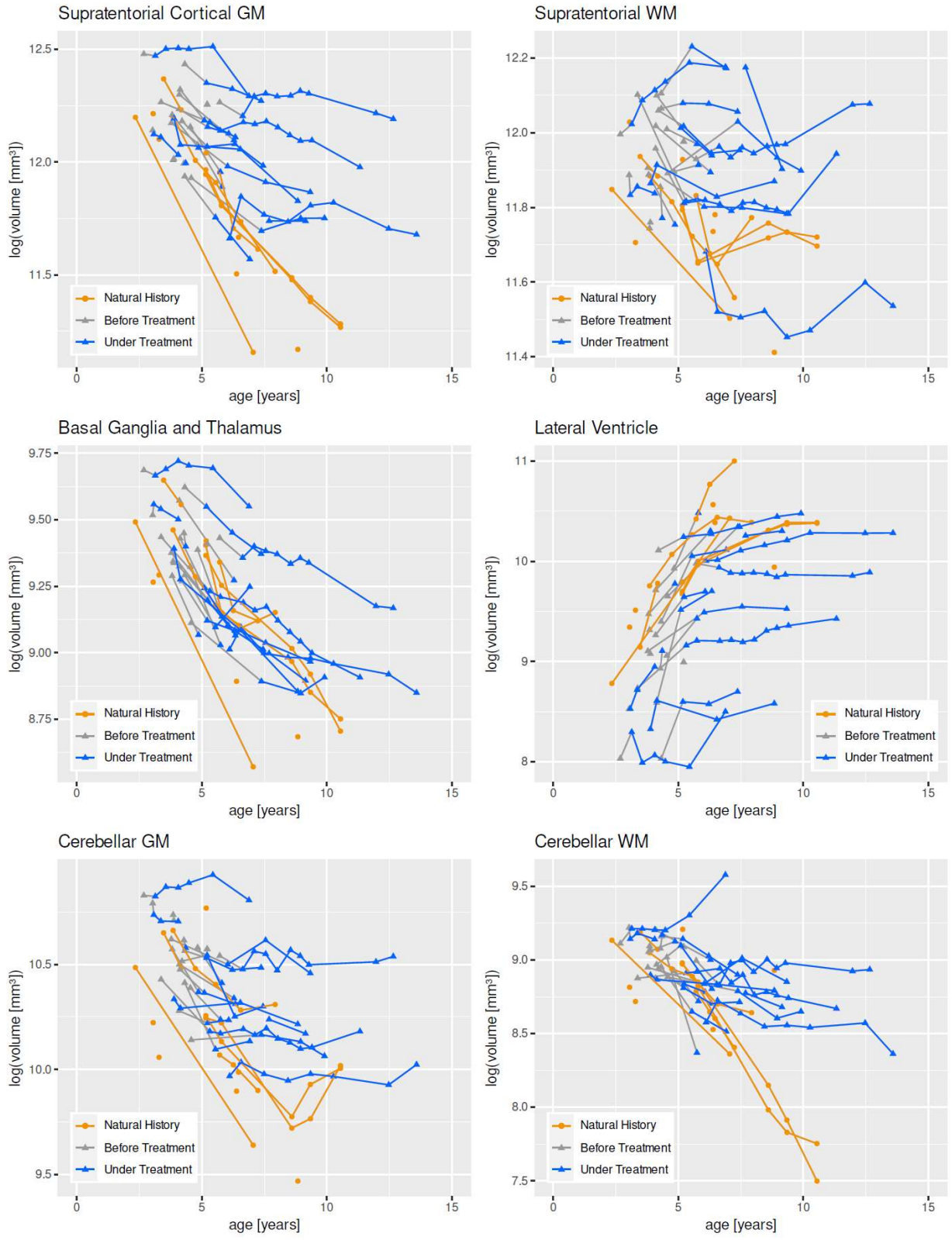

FIG 2. Brain volumes of CLN2 patients treated enzyme replacement therapy. A reduced rate of cerebral volume loss is demonstrated across the supratentorial and infratentorial white and grey matter in our patients (blue triangles) compared to a natural history cohort (yellow dots, average of both hemispheres). Grey triangles depict MRI scans of our treatment cohort before ERT. A slower rate of increase in volume of lateral ventricles is also shown.

Statistical analysis of brain volume changes correlated with age in treated (left and middle columns) and untreated CLN2 patients (right column) patients is shown in Supplementary Table 2. The treatment cohort has been analysed for the baseline to year follow-up (left columns) and change during follow-up only (middle columns). All segmented brain regions of the treatment cohort during the follow-up period excluding the baseline scans (Supplementary Table 2, middle rows; Figure 2, blue symbols, and lines) showed a much slower rate of volume loss compared to the natural history cohort. The reduction rates of brain volumes in our treatment cohort (compared to the natural history cohort) per year were: Supratentorial cortical grey matter 3% (vs 16.8%), supratentorial white matter 0.23% (vs 6.3%), cerebellar grey matter 1% (vs 10.1%), cerebellar white matter 3.8 % (vs 17.2%) and basal ganglia/thalami 4.4% (vs 12.5%). The lateral ventricles showed a slower rate of increase in volume of 3.5% annually (vs 25.9%). A significant change of volume loss between our cohort and the natural history cohort was observed for supratentorial cortical grey matter (13.8% difference), cerebellar white matter (13.4%) and cerebellar grey matter (9.1%). However, the difference was greatest for the lateral ventricles where the difference in volume increase was reduced by 22.4%. Of these regions, supratentorial cortical grey matter showed the lowest error of the estimated volume change rate making it most reliable. The reduced Pearson's correlation coefficients compared to the natural history cohort also demonstrate the effectiveness of treatment (Supplementary Table 2, middle rows). Importantly, on treatment, when there is minimal to no volume loss, as is the case for the supratentorial white matter region, the volume change rate and the Pearson's correlation coefficient are close to zero and therefore do not reach statistical significance, with p values of more than 0.05.

The correlation analysis of the supratentorial grey matter volume with the available clinical scores (Figure 3) showed a high correlation with $r = 0.71$ ($p<0.001$). Three patients showed a volume loss with no change of the clinical scores (vertical lines, patients C1, D2 and G1) and one patient showed a decline of the clinical scores but a slight increase in volume (patient A2).

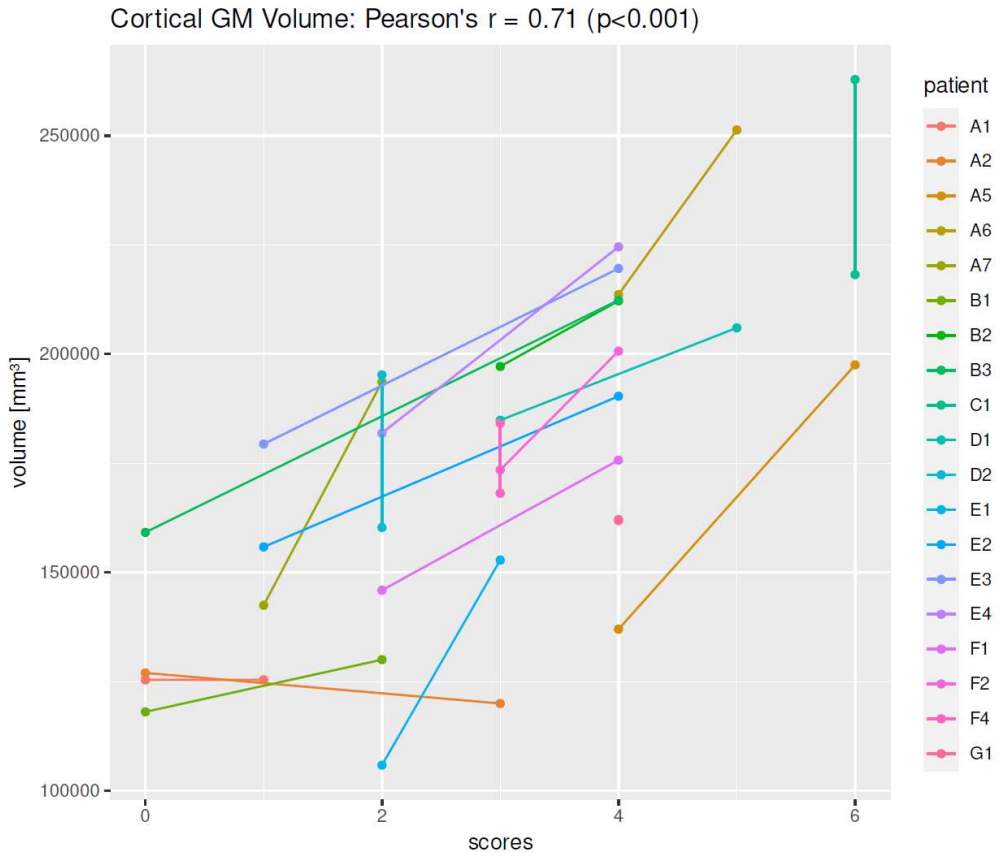

FIG 3. Correlation analysis between the clinical scores (motor and language) and cortical GM volumes. These were compared for the closest MRI scan date from the date of clinical score assessment (Table 1). The clinical scores and volume measurements are highly correlated with each other; cortical GM volume can be used as a surrogate marker for the clinical scores.

DISCUSSION

This study analyzed segmented MRI brain volumes of CLN2 patients on ERT. In comparison to a natural history cohort of untreated patients, brain volume loss was significantly reduced in all brain regions in the follow-up period with the patients already one year on treatment which included supratentorial grey and white matter, infratentorial grey and white matter and basal ganglia/thalami. The strongest difference in volume decline with age compared to the natural history cohort was observed for supratentorial grey matter with an annual 13.8% reduction in volume loss. Volume loss in the cerebellar white matter was reduced by 13.4% and by 9.1% in the cerebellar grey matter volumes. Basal ganglia/thalami and supratentorial white matter showed a 7.7% and 6.1% difference, respectively. Interestingly, a

strong difference between the two cohorts was also seen for the size of the lateral ventricles where the difference in annual volume increase was 22.4%. Our results suggest that MRI volumetry is useful for quantitative treatment monitoring.

Artefact on imaging limits accurate volumetric assessment; all the patients had ICV reservoirs which are used for ERT administration and were a source of significant susceptibility artefact. We were able to demonstrate, using statistical analysis of the natural history cohort, that it is possible to rely on one hemisphere only for data analysis. As previously shown,[6] volumetry is a sensitive marker of disease progression as marked by continued volume loss despite scoring a 'zero' on the clinical rating score. Correlation analysis between the clinical scores (motor and language) and cortical GM volumes (Figure 3) revealed that clinical scores and volume measurements are highly correlated with each other; cortical GM volume can be used as a surrogate marker for the clinical scores. Overall, the volume loss is correlated with a decline in clinical scores. Additionally, our current data shows continued volume loss despite persistent high clinical scores (patients C1, D2 and G1), indicating that even in early stages of disease where there is no clinical progression, MRI is already primed and more sensitive to disease progression and treatment response. Our study adds new knowledge to prior literature by demonstrating the MRI is a more sensitive biomarker compared with clinical scores, by processing regional anatomical and volumetric analysis as well as encapsulating imaging changes prior to clinical deterioration.

Our results are also in agreement with the slowed rate in decline of motor and language function of CLN2 patients on ERT during the initial clinical trial,[23] Schulz et al.[5] demonstrated a slowed rate of clinical score measuring motor and speech decline. In addition, among the treated patients, the annual rate of loss of total grey matter volume over a 96-week period was 6.7%, with larger decreases seen during the first year of treatment compared to the remainder of the period of analysis.[5] In our cohort, grey matter volumes showed slightly less reduction annually with 3%.

Previous studies in non-treated patients have also demonstrated that MRI volumetry provides a sensitive biomarker for monitoring disease progression in CLN2 disease.[6, 22] The most rapid volume loss has been observed for the cerebrum, followed by thalamus and cerebellum, dropping out of the normal range between 6 months- 3 years of age.[22] Therefore, it may not be surprising that supratentorial and infratentorial grey matter showed the strongest difference in annual decline between treated and non-treated cohorts. The annual decrease in supratentorial cortical grey matter in untreated patients 16.8% reduced to only 3%. Interestingly, cerebellar white matter, which showed an annual volume loss of 17.2% in untreated patients, also decreased to only 3.8% in the ERT cohort. This is an interesting finding since the loss of axons and myelin sheaths in the cerebellar and cerebral white matter is believed to be a secondary effect to the loss of granular and Purkinje cells in the cerebellum and loss of cortical neurons.[9] It may be that the rate of cerebellar white matter volume loss was much improved in the ERT cohort compared to the natural history cohort, since in the latter there is not only direct secondary Wallerian degeneration via loss of axons through cerebellar grey matter loss, but also secondary diaschisis of the white matter tracts secondary to interruption of the cortico-pontine-cerebellar tracts resulting in hypometabolism of the cerebellum.[9, 10]

There were a few limitations of our study. The imaging parameters and scanners of the datasets varied for our patients due to the retrospective nature of the data collection. This can lead to variability of segmentation and, therefore, statistical analysis (Supplementary Table 2). Another limitation was the use of variable 1.5T and 3 T scanners, which can lead to subtle differences in detection of atrophy and thus affect overall volume prediction with 3T being better at detecting small changes in volume.[25] However, we expect little effect on our results as most scans were done on 1.5T scanners. Amongst other limitations were the signal dropout from the ICV however this was countered by using only the contralateral hemisphere which was statistically proven no different to the contralateral side. A such, the patients were also included into the protocol at different stages during their disease, introducing a variability in baseline neurodegeneration at the point of treatment commencement.

For future directions, it would be prudent to standardize imaging protocols and perform scans on equivalent Tesla MR scanners. Furthermore, it would be interesting to analyze the inherent T1- and T2-weighted images intensities, or quantitative parameters such as MR spectroscopy, quantitative susceptibility mapping or myelin water imaging to assess more subtle changes of disease progression and treatment response.

CONCLUSIONS

MRI volumetry is an effective tool to quantitatively evaluate disease progression and assess the efficacy of treatment, demonstrating higher sensitivity than current clinical biomarkers. Our results have analyzed the rate of volume decline in several structures of the brain, which is novel compared to prior research in this field. The patients on ERT showed a significant reduction in cerebral volume loss in comparison to the natural history cohort.

ACKNOWLEDGMENTS

Sincere thanks to the NCL clinic at the University Medical Center Hamburg-Eppendorf, Hamburg, Germany.

REFERENCES

1. Nita DA, Mole SE, Minassian BA. Neuronal ceroid lipofuscinoses. Epileptic Disord. 2016 Sep 1;18(S2):73-88. doi: 10.1684/epd.2016.0844.
2. Kaminiów K, Kozak S, Paprocka J. Recent Insight into the Genetic Basis, Clinical Features, and Diagnostic Methods for Neuronal Ceroid Lipofuscinosis. Int J Mol Sci. 2022 May 20;23(10):5729. doi: 10.3390/ijms23105729.
3. Sleat DE, Donnelly RJ, Lackland H et al . Association of mutations in a lysosomal protein with classical late-infantile neuronal ceroid lipofuscinosis. Science. 1997 Sep 19;277(5333):1802-5. doi: 10.1126/science.277.5333.1802
4. Mukherjee, A.B., Appu, A.P., Sadhukhan, T. et al. Emerging new roles of the lysosome and neuronal ceroid lipofuscinoses. Mol Neurodegeneration 14, 4 (2019). https://doi.org/10.1186/s13024-018-0300-6
5. Schulz A, Ajayi T, Specchio N et al CLN2 Study Group. Study of Intraventricular Cerliponase Alfa for CLN2 Disease. N Engl J Med. 2018 May 17;378(20):1898-1907. doi: 10.1056/NEJMoa1712649
6. Löbel U, Sedlacik J, Nickel M et al Volumetric Description of Brain Atrophy in Neuronal Ceroid Lipofuscinosis 2: Supratentorial Gray Matter Shows Uniform Disease Progression. AJNR Am J Neuroradiol. 2016 Oct;37(10):1938-1943. doi: 10.3174/ajnr.A4816.
7. D'Incerti L. MRI in neuronal ceroid lipofuscinosis. Neurol Sci. 2000;21(3 Suppl):S71-3. doi: 10.1007/s100720070043
8. Aydın K, Havali C, Kartal A, Serdaroğlu A, Haspolat Ş. MRI in CLN2 disease patients: Subtle features that support an early diagnosis. Eur J Paediatr Neurol. 2020 Sep;28:228-236. doi: 10.1016/j.ejpn.2020.07.009.
9. Vanhanen SL, Raininko R, Santavuori P et al. MRI evaluation of the brain in infantile neuronal ceroid-lipofuscinosis. Part 1: Postmortem MRI with histopathologic correlation. J Child Neurol. 1995 Nov;10(6):438-43. doi: 10.1177/088307389501000603.
10. Biswas A, Krishnan P, Amirabadi A, Blaser S, Mercimek-Andrews S, Shroff M. Expanding the Neuroimaging Phenotype of Neuronal Ceroid Lipofuscinoses. AJNR Am J Neuroradiol. 2020 Oct;41(10):1930-1936. doi: 10.3174/ajnr.A6726.
11. Vanhanen SL, Raininko R, Autti T et al. MRI evaluation of the brain in infantile neuronal ceroid-lipofuscinosis. Part 2: MRI findings in 21 patients. J Child Neurol. 1995 Nov;10(6):444-50. doi: 10.1177/088307389501000604.
12. Autti T, Joensuu R, Aberg L. Decreased T2 signal in the thalami may be a sign of lysosomal storage disease. Neuroradiology. 2007 Jul;49(7):571-8. doi: 10.1007/s00234-007-0220-6. Epub 2007 Mar 3.
13. Chang M, Cooper JD, Sleat DE et al. Intraventricular enzyme replacement improves disease phenotypes in a mouse model of late infantile neuronal ceroid lipofuscinosis. 2008 Feb 12. PMID: 18362923.
14. Vuillemenot BR, Kennedy D, Cooper JD et al. Nonclinical evaluation of CNS-administered TPP1 enzyme replacement in canine CLN2 neuronal ceroid lipofuscinosis. Mol Genet Metab. 2015 Feb;114(2):281-93. doi: 10.1016/j.ymgme.2014.09.004. Epub 2014 Sep 16. PMID: 25257657.
15. Schulz A, Specchio N, de Los Reyes E et al. Safety and efficacy of cerliponase alfa in children with neuronal ceroid lipofuscinosis type 2 (CLN2 disease): an open-label extension study. Lancet Neurol. 2024 Jan;23(1):60-70. doi: 10.1016/S1474-4422(23)00384-8.
16. http://www.bdfa-uk.org.uk/research-and-resources/brineura-for-cln2/- Accessed 25th February 2024.
17. Dyke JP, Sondhi D, Voss HU et al. Brain Region-Specific Degeneration with Disease Progression in Late Infantile Neuronal Ceroid Lipofuscinosis (CLN2 Disease). AJNR Am J Neuroradiol. 2016 Jun;37(6):1160-9. doi: 10.3174/ajnr.A4669.
18. Hochstein JN, Schulz A, Nickel M, et al. Natural history of MRI brain volumes in patients with neuronal ceroid lipofuscinosis 3: a sensitive imaging biomarker. Neuroradiology. 2022 Oct;64(10):2059-2067. doi: 10.1007/s00234-022-02988-9.
19. Knoernschild, K., Johnson, H.J., Schroeder, K.E. et al. Magnetic resonance brain volumetry biomarkers of CLN2 Batten disease identified with miniswine model. Sci Rep 13, 5146 (2023). https://doi.org/10.1038/s41598-023-32071-z
20. Bates D, Mächler M, Bolker B, Walker S. Fitting Linear Mixed-Effects Models Using lme4. J Stat Softw. 2015;67(1).
21. Kim S. ppcor: An R Package for a Fast Calculation to Semi-partial Correlation Coefficients. Commun Stat Appl Methods. 2015 Nov;22(6):665–74.
22. Baker EH, Levin SW, Zhang Z, et al MRI Brain Volume Measurements in Infantile Neuronal Ceroid Lipofuscinosis. AJNR Am J Neuroradiol. 2017 Feb;38(2):376-382. doi: 10.3174/ajnr.A4978.
23. Nickel M, Simonati A, Jacoby D et al. A. Disease characteristics and progression in patients with late-infantile neuronal ceroid lipofuscinosis type 2 (CLN2) disease: an observational cohort study. Lancet Child Adolesc Health. 2018 Aug;2(8):582-590. doi: 10.1016/S2352-4642(18)30179-2.
24. Fischl B. FreeSurfer. Neuroimage. 2012 Aug 15;62(2):774–81
25. Chow N, Hwang KS, Hurtz et al; Alzheimer's Disease Neuroimaging Initiative. Comparing 3T and 1.5T MRI for mapping hippocampal atrophy in the Alzheimer's Disease Neuroimaging Initiative. AJNR Am J Neuroradiol. 2015 Apr;36(4):653-60. doi: 10.3174/ajnr.A4228.

SUPPLEMENTAL FILES

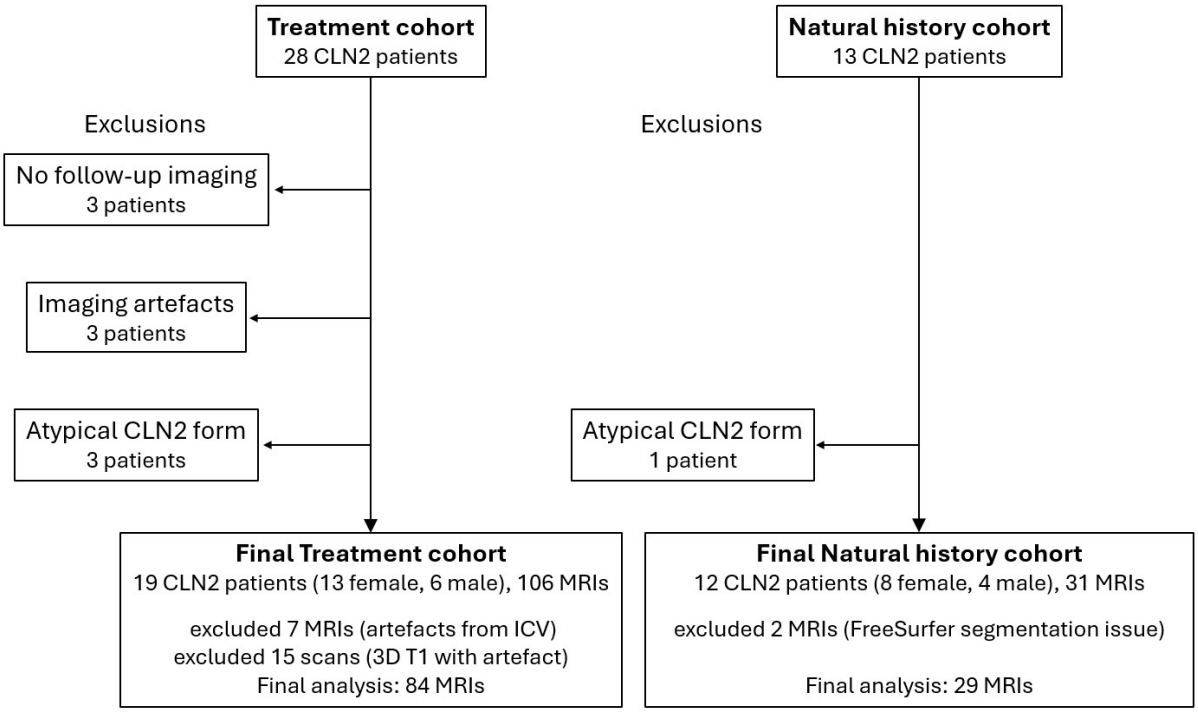

Supplementary Fig 1: Flow chart representing patient inclusion and exclusion criteria.

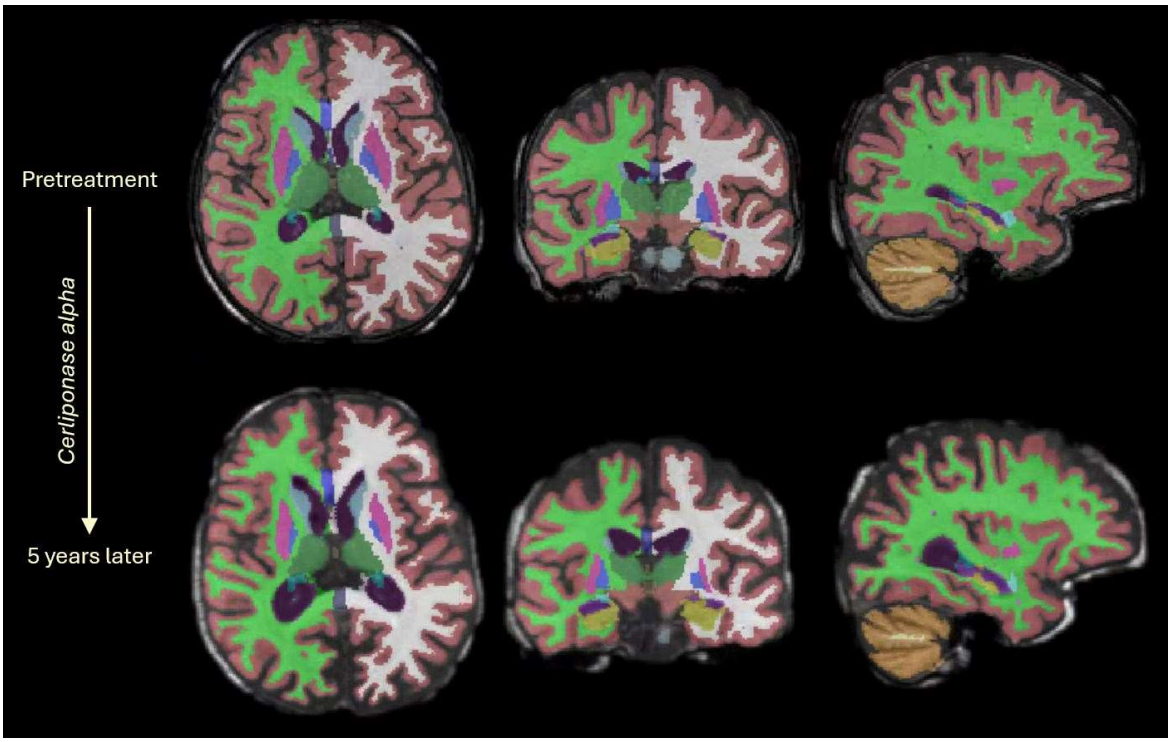

Supplementary Fig 2.1: Exemplary brain volume segmentation of 4-year patient before and after 5 years of enzyme replacement therapy.

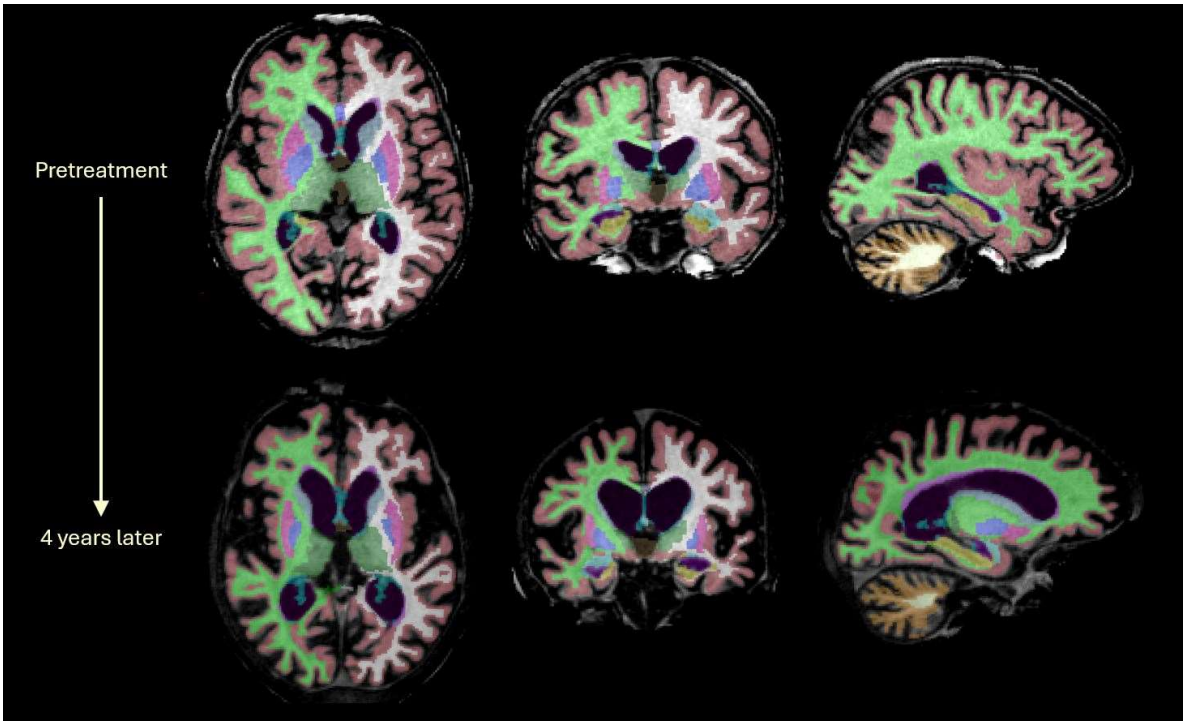

Supplementary Fig 2.2: Exemplary brain volume segmentation of a 5-year-old patient from the natural history cohort (no treatment) at baseline and 4 years later. The marked degree of global volume loss is evident.

Supplementary Table 1: Patient characteristics including age at first MRI, clinical phenotype and genetic mutations identified for the natural history cohort.

Patient ID	**Age at 1st MRI** [years]	**Phenotype**	**Mutation**
CLN2_065_1_100_03	8.8	late infantile	c.622C>T / c.622C>T
CLN2_455_1_041_01	3.5	late infantile	c.622C>T / c.509-1G>C
CLN2_457_1_042_01 (twin 1)	5.2	late infantile	c.1094G>A / c.1094G>A
CLN2_457_2_080_01 (twin 2)	5.2	late infantile	c.1094G>A / c.1094G>A
CLN2_467_1_047_02	13.8	atypical	c.1439T>G / c.509-1G>C
CLN2_468_1_017_01	3.8	late infantile	c.622C>T / c.509-1G>C
CLN2_473_1_088_01	5.7	late infantile	c.311T>C / IVS 5-1G>C
CLN2_479_1_01	2.3	late infantile	c.622C>T / c.622C>T
CLN2_481_1_101_01	6.4	late infantile	c.622C>T / c.622C>T
CLN2_486_1_01	3.3	late infantile	c.509-1G>C / c.833A>G
CLN2_495_1_01	5.2	atypical	c.380G>A / c.509-1G>C
CLN2_499_1_01	6.5	late infantile	c.230-13T>A / c.622C>T
CLN2_999_1_01	3.1	late infantile	c.622C>T / c.622C>T

Supplementary Table 2: Statistical analysis of brain volume changes in treated and untreated CLN2 patients (right columns). The volume change rate from the linear mixed-effects model is reported in percent volume change per year and the Pearson correlation coefficient (r) is reported for the correlation with age. The treatment cohort has been analysed for the baseline to first year follow-up (left columns) and change during follow-up only (middle columns).

	Baseline - 1 year follow-up on treatment (11 patient, 25 observations)		**Treatment** (only follow-ups 1-9y) (19 patients, 65 observations)		**Natural history cohort** (12 patients, 56 observations)	
Segmented brain region	**Volume change rate over the first year only**	**Correlation with age over the first year only**	**Volume change rate** (% per year)	**Correlation with age** (Pearson)	**Volume change rate** (% per year)	**Correlation with age** (Pearson)
Supratentorial Cortical grey matter	-11 ± 1.8 (p<0.001)	r = -0.45 (p<0.05)	-3.0 ± 0.74 (p<0.001)	r = -0.39 (p<0.01)	-16.8 ± 1.5 (p<0.001)	r = -0.92 (p<0.001)
Supratentorial white matter	-1.6 ± 2.3 (p=0.24)	r = 0.099 (p=0.64)	0.23 ± 0.65 (p=0.37)	r = 0.28 (p=0.27)	-6.3 ± 1.9 (p<0.01)	r = -0.54 (p<0.001)
Basal Ganglia/ Thalami	-13 ± 2 (p<0.001)	r = -0.67 (p<0.001)	-4.8 ± 1.3 (p<0.001)	r = -0.62 (p<0.001)	-12.5 ± 1.5 (p<0.001)	r = -0.82 (p<0.001)
Lateral Ventricle	41 ± 7.3 (p <0.001)	r = 0.74 (p<0.001)	3.4 ± 1.0 (p<0.01)	r = 0.54 (p<0.001)	25.9 ± 5.0 (p<0.001)	r = 0.69 (p<0.001)
Cerebellar grey matter	-11 ± 2.3 (p<0.001)	r = -0.7 (p<0.001)	-1.0 ± 0.44 (p<0.05)	r = -0.48 (p<0.001)	-10.1 ± 2.2 (p<0.001)	r = -0.67 (p<0.001)
Cerebellar white matter	-14 ± 3.7 (p< 0.01)	r = -0.68 (p<0.001)	-3.8 ± 1.6 (p<0.05)	r = -0.52 (p<0.001)	-17.2 ± 3.1 (p<0.001)	r = -0.84 (p<0.001)